SSC22-WKI-09

A High Precision Accelerometer with an Optical Readout

Abdulrahman Alfauwaz
King Abdulaziz City for Science and Technology
Al Raed, Riyadh 11442, Saudi Arabia; +966-505243874
alfawwaz@kacst.edu.sa

Sasha Buchman, John Lipa
Stanford University
Stanford, California 94305, United States; +1-6508234905
sbuchman@stanford.edu

ABSTRACT

Geodesic missions require precise accelerometers to improve the knowledge of the reference frame used for defining position coordinates, better calculating orbit parameters, and mapping the Earth's gravitational field. Although space environment disturbances are typically relatively small, they generate large and significant accumulated drift errors over time. We describe a low noise accelerometer design that overcomes many of the limitations of existing designs and is capable of providing precision drag-free control in vehicles with thrusters. Furthermore, it can be used with some modifications, including active thermal control, to detect gravitational waves in an interferometer using drag-free satellites. Due to its flexible design requirements for volume, weight, and power, our proposed instrument can be accommodated in small satellites.

INTRODUCTION

In general, space missions that aim to measure Earth's gravitational field and satellites that are used in navigational applications, to increase its level of accuracy, require a device that can measure acceleration. Accelerometers are actively under development for space applications.[1,2] They usually use a test mass (TM) which has a cube or plate shape in conjunction with a capacitive displacement sensor.[3] However, although the performance of this design has improved over years of development, it still exhibits some limiting factors.[4] The most significant limitation is the measurement of the TM displacement. For capacitive readouts the displacement sensitivity decreases with increasing gap separation between the TM and its housing. A large gap size is however desirable, since the disturbance forces on the TM decrease by as much as the third power of the gap size. Due to their cube-like TM design, these accelerometers, or drag-free sensors, also have additional significant electrostatic disturbance forces exerted on the TM, the back action generated by their suspension and capacitive readout systems.

In this paper we propose a High-Precision Accelerometer (HPA) based on a low-noise spherical TM design that involves a simpler control system, is ideally suited for an optical-based readout, and can accommodate large gaps of the order of the TM radius. Large gaps reduce sensitivity to TM charges and patch effects, magnetic susceptibility, mass imbalance, and non-sphericity.

The optical readout is based on a differential optical shadow sensor (DOSS), a highly precise system that measures the displacement of the TM relative to its housing; defined as the reference system.[6] The dynamic range of the DOSS is larger compared to current accelerometer readout systems and will provide a significant reduction in the cost, volume, weight, and power of missions, while adding flexibility to their design requirements. Included in the design is an UV-LED based charge management system, required for maintaining the TM charge close to ground potential.[7] The proposed accelerometer has an initial performance capability goal of acceleration less than 10^{-10} ms^{-2} = 10^{-8} Gal.

In addition to geodesic missions, this instrument can also serve as the reference sensor for drag-free missions, when thrusters are available. Furthermore, it can be used with some modifications, including active thermal control, to detect gravitational waves in an interferometer using drag-free satellites.[11] Due to its flexible design requirements for volume, weight, and power, our proposed instrument can be accommodated in small satellites.

ACCELEROMETER

In most accelerometers, the TM having the shape of a cube or plate allows several advantages. These

advantages apply mainly to capacitive and interferometric sensors.[4,5] A spherical shape is also common for the TM and provides several advantages for the use of optical sensors. An advantage of the spherical design is in not requiring rotational control so that the servo control is implemented in three rather than in six degrees of freedom. In contrast, for the capacitive position measurement for a spherical TM with large gap, the accuracy and linearity are poor, and the crosstalk between different axes is significant.[8] Note that a spherical TM cannot be used to monitor the rotational motions of a satellite.

To improve the performance of accelerometers, we must minimize or eliminate the noises from the various disturbance sources. Figure 1 shows a schematic of the system network and how the major subsystems communicate with each other. Thermal noise control will improve the position measurement at low frequency. Centering system noise will be minimized by increasing the gap between the TM and housing. Electronic noise will be minimized by careful design of the electronics to the requirement of the instrument.

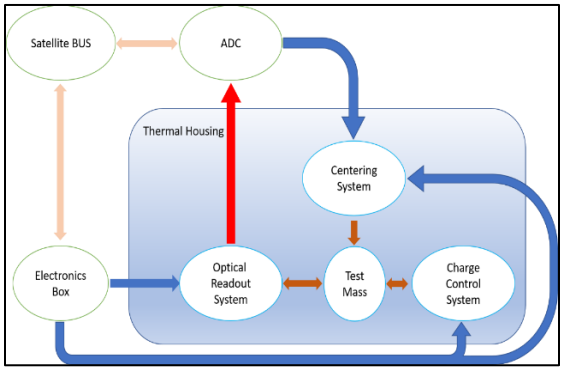

Figure 1 Schematic of Network of Subsystems.

Optical Readout System

The optical readout system presented is based on a Differential Optical Shadow Sensor (DOSS), which uses 8 TM-grazing beams (see figure 2) to determine the position of the spherical, 2.5 cm diameter, beryllium copper TM. A prototype of the DOSS was developed for our Modular Gravitational Reference Sensor (MGRS) in the exact form and function factor as for the proposed instrument.[1] The achieved performance, shown in figure 3, exceeds the goal for the drag-free instrument and is about 2 nm·Hz$^{-½}$ in the frequency region of interest above 0.5 Hz.

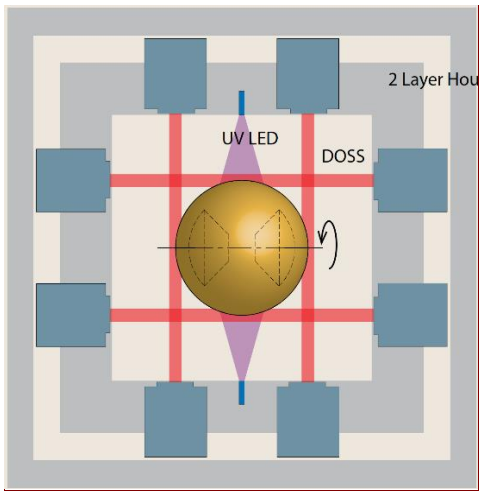

Figure 2 DOSS and UV-LED schematics.

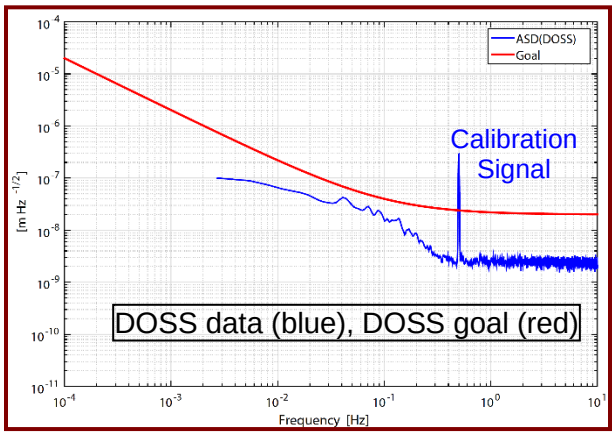

Figure 3 DOSS Performance.

Centering "Suspension" System

For the maximum nominal spacecraft acceleration of 10^{-7} ms^{-2} Hz$^{-½}$ the bandwidth of the suspension system will have to be above 0.5 Hz. We plan to use a 0.5 Hz system, similar to that the one for the Relativity Mission, Gravity Probe B (GP-B).[9] Six suspension electrodes with a r_e = 1.25 cm radius each, in three orthogonal pairs on the faces of the cubic housing, will have a $d_0 \approx 1$ cm spacing and a capacitance of about 1 pF to the TM. For the m = 0.070 Kg mass of the TM, the force, acceleration, and voltage required to be provided by one electrode are given by:

$$F_P \equiv a_P m = \frac{C_0}{d_0} V_P^2, \quad a_P \leq 10^{-6} m \cdot s^{-2}, \quad V_P = \sqrt{a_P m \frac{d_0}{C_0}} \cong 27\text{V} \qquad (1)$$

Thus V_P, the preload voltage of the suspension system in operational mode, will be 27 V, with a secondary 100 V preload for TM levitation, capture, and initialization. The suspension voltage change δV_e corresponding to the 10^{-10} ms^{-2} detection requirement is given by (for two electrodes on one axis):

$$\delta V_e = \frac{V_{PL}}{4} \cdot \frac{a_{DFPA}}{a_P} \approx 1 \text{ mV} \qquad (2)$$

an easily achievable measurement level.

The GP-B Gyro Suspension System (GSS) is our heritage technology for the HPA electro-static suspension.[9] The GSS was fully demonstrated in flight. Unlike the HPA, the GSS was required to operate both in flight and in ground test covering an operational range of over 9 orders of magnitude. Table 1 compares a summary of the GP-B GSS functions with the much simpler HPA requirements. Note that all difficult requirements and much of the functionality (including the high voltage ground suspension) are not needed, thus requiring only a very simple version of the GSS for the HPA. This enables size, weight, and power savings to be realized on HPA. Table 1 gives a comparison of the requirements for the GP-B and HPA suspension systems, illustrating the major simplifications of the HPA versus the GP-B electronics.

Table 1 Electrostatic suspension system requirements: GP-B flight versus HPA

Requirement / System	GP-B (2004-2005 flight)	HPA
Resolution as accelerometer	$< 10^{-12}$ g	$< 10^{-11}$ g
Suspension system	Hybrid digital/analog	Digital only
Operational range	10^{-9} g to 1 g (0.05 V -1,000 V) (9 orders of magnitude)	10^{-8} g to 10^{-7} g (24 V – 100 V) (2 orders of magnitude)
Adaptive control algorithm	Adaptive LQE digital control	Not required; PDI only
Backup TM suspension system	3 backup, analog PD controllers	Not required
TM position sensing	Capacitive to 0.15 nm/√Hz	Not required (see DOSS)
TM spin alignment	Preload modulation at SC roll	Not required
TM charge measurement	3 axes force modulation	Not required

Charge Control System

The TM will charge during the mission via two main mechanisms.

a) During levitation the separation of two conductive surfaces causes charging of the TM trough the triboelectric effect.
b) Cosmic radiation causes charged particles to be stopped in the TM.

TM non-contact charge management was first flight demonstrated by GP-B using photoelectrons generated by the 254 nm line of a mercury lamp discharge.[10] In 2014, Stanford, in collaboration with NASA and KACST, has launched the UV-LED mission and demonstrated in space charge management using gallium nitride UV-LEDs with a center wavelength of 255 nm and 10 nm FWHM.[2] The MGRS and HPA will use a similar system. Table 2 gives the flight and ground development heritage track for the HPA through the DISCOS (1974), the GP-B (2004), and the UV-LED (2014) missions, and the MGRS and HPA instruments development.

Thermal Control of TM Housing

The HPA housing consists of two layers of aluminum separated by vacuum with supporting spacers of low thermal conductivity in between. The outer layer is 5 mm thick and connects to the spacecraft bus interface plate through a low thermal conductivity adapter ring, while the inner layer (the TM housing) is 2 cm thick and is supported by the low-conductivity spacers.

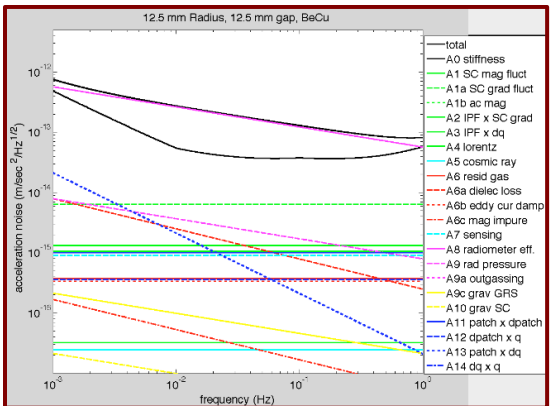

Figure 4 MGRS acceleration noise error tree.

The largest contribution to the thermal disturbance budget is the radiometer effect (pink line A8 in figure 4, above). Residual gas pressure in the HPA is about 10^{-4} Pa and the system requirements for temperature fluctuations and gradients are ≤ 50 mK. Temperature control is achieved with a double enclosure system, which is identical to the MGRS design.[11] Note that the MGRS requires active temperature control for noise performance at the 10^{-12} ms^{-2} Hz$^{-1/2}$ level, while the HPA does not, as a passive thermal control is more than sufficient for the 10^{-10} ms^{-2} Hz$^{-1/2}$ design performance level. This allows for mass and power savings for HPA while still exceeding performance requirements. Figure 5 shows a CAD drawing of the two-layer prototype HPA design while figure 6 shows the laboratory model of the MGRS thermal enclosure.

Table 2 Flight heritage track of main HPA systems (cells in gray)

	DISCOS (1974)	GP-B (2004)	UV-LED (2014)	MGRS	HPA
Performance	5×10^{-11} ms^{-2} RMS	10-9 ms-2Hz-½	N/A	10^{-12} ms^{-2}Hz$^{-½}$	10^{-10} ms^{-2}Hz$^{-½}$
TM	20 mm ϕ, AuPt	38 mm ϕ, quartz	N/A	25 mm ϕ, BeCu	25 mm ϕ, BeCu
TM housing	40 mm, 1 layer	38.06 mm 1 layer	N/A	50 mm 2 layer	50 mm 2 layer
Caging	Mechanical	N/A	N/A	Mechanical	Mechanical
TM position	Capacitance	Capacitance	N/A	DOSS	DOSS
Suspension	N/A	Electrostatic	N/A	N/A	Electrostatic
Thermal ctrl.	Passive	Low temp, active	N/A	Active 2 layer	Passive 2 layer
Charge mgmt.	Wall contact	UV Hg active	UV-LED	UV-LED	UV-LED

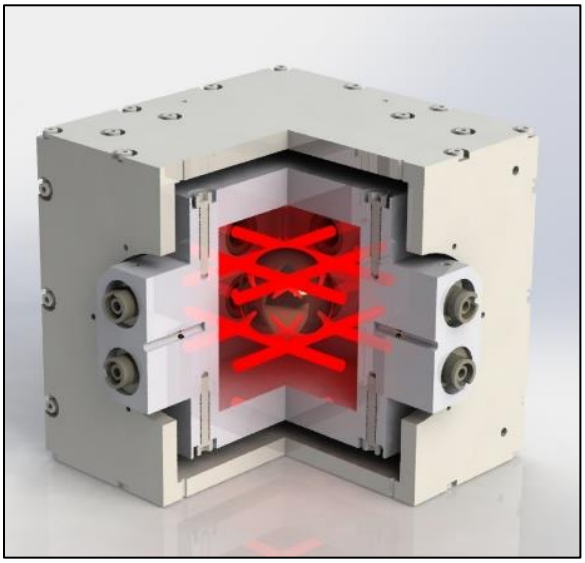

Figure 5 The MGRS Proposed Setup

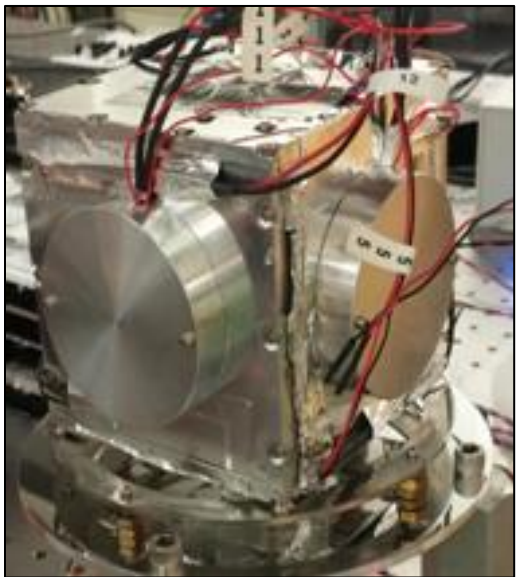

Figure 6 The MGRS thermal enclosure

PROTOTYPE MODEL

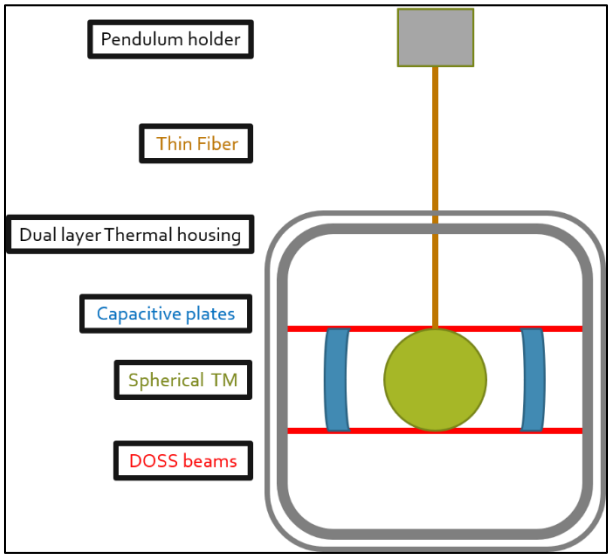

Figure 7 Laboratory Prototype model.

The laboratory test model consists of a pendulum and its holder suspending the TM by a thin fiber which made of tungsten. Its length which is 1 meter is intended to minimize the horizontal restoring force for small displacements. A schematic view is shown in Figure 7.

CONCLUSION

The HPA needs to be validated, and therefore we are planning design and build a high-fidelity simulator that can replicate all error sources. The simulator will help optimize the HPA and allow us to make any necessary modifications. Moreover, the prototype model will also confirm the performance of the HPA. The simulator and prototype model will support achieving the initial goal of measuring acceleration with a precision of $\leq 10^{-10}$ ms^{-2} $=10^{-8}$ Gal with the HPA. Longer term the design can be upgraded to meet a performance goal of $\sim 10^{-12}$ ms^{-2} $= 10^{-10}$ Gal.

Acknowledgments

We would like to thank the W.W. Hansen Experimental Physics Laboratory at Stanford University for their support. We are indebted to Professor Simone D'Amico, the Founding Director of the Space Rendezvous Lab (SLAB), for his helpful feedback and valuable comments.

References

1. B. Christophe, D. Boulanger, B. Foulon, P.-A. Huynh, V. Lebat, F. Liorzou, E. Perrot, "A new generation of ultra-sensitive electrostatic accelerometers for GRACE Follow-on and towards the next generation gravity missions", Acta Astronautica, vol. 117, 2015, pages 1-7, https://doi.org/10.1016/j.actaastro.2015.06.021.
2. Bock, H., Jäggi, A., Beutler, G. et al. "GOCE: precise orbit determination for the entire mission", J Geod 88, 1047–1060 (2014). https://doi.org/10.1007/s00190-014-0742-8.
3. Sarra, P., "Integration and Testing of the Inertial Sensor for LISA Pathfinder mission", 40th COSPAR Scientific Assembly, vol. 40, 2014.
4. Armano, Michele et al, "Sub-Femto- g Free Fall for Space-Based Gravitational Wave Observatories: LISA Pathfinder Results", Physical Review Letters. 116. 10.1103/PhysRevLett.116.231101.
5. Enrico Canuto, "Drag-free and attitude control for the GOCE satellite", Automatica, vol. 44, issue 7, 2008, pages 1766-1780, https://doi.org/10.1016/j.automatica.2007.11.023.
6. Andreas Zoellner, Si Tan, Shailendhar Saraf, Abdul Alfauwaz, Dan DeBra, Sasha Buchman, and John A. Lipa, "Differential optical shadow sensor for sub-nanometer displacement measurement and its application to drag-free satellites," Opt. Express 25, 25201-25211 (2017)
7. Shailendhar, Saraf et al "Ground testing and flight demonstration of charge management of insulated test masses using UV-LED electron photoemission" 2016 Class. Quantum Grav. 33 245004
8. Touboul, P., Foulon, B., and Willemenot, E., "Electrostatic space accelerometers for present and future missions", Acta Astronautica, vol. 45, no. 10, pages 605–617, 1999. doi:10.1016/S0094-5765(99)00132-0.
9. Keiser GM, Buchman S, Bencze W, DeBra DB., "The expected performance of Gravity Probe B electrically suspended gyroscopes as differential accelerometers". AIP Conference Proceedings 1998 Dec 14 (pp. 188-198). IOP INSTITUTE OF PHYSICS PUBLISHING LTD https://doi.org/10.1063/1.57411
10. Buchman Saps, Quinn Theodore, Keiser G. M., Gill Dale, and Sumner T. J., "Charge measurement and control for the Gravity Probe B gyroscopes", Journal of Review of Scientific Instruments, vol. 66, No 1, 1995.
11. Alfauwaz, Abdulrahman et al, "Thermal Control of a Gravitational Reference Sensor", 46th AIAA Thermophysics Conference